



日本原子力研究開発機構機関リポジトリ
Japan Atomic Energy Agency Institutional Repository

| | |
|--------------|-------------------------------------------------------------------------------------------------------------------------------------|
| Title | Beam monitors for the commissioning of energy upgraded linac |
| Author(s) | Miura Akihiko, Maruta Tomofumi, Liu Y., Miyao Tomoaki, Kawane Yusuke, Ouchi Nobuo, Oguri Hidetomo, Ikegami Masanori, Hasegawa Kazuo |
| Citation | JPS Conference Proceedings, 8,p.011002_1-011002_6 |
| Text Version | Author's Post-print |
| URL | https://jopss.jaea.go.jp/search/servlet/search?5047407 |
| DOI | https://doi.org/10.7566/JPSCP.8.011002 |
| Right | ©2015 The Physical Society of Japan |

Beam Monitors for the Commissioning of Energy Upgraded Linac

Akihiko MIURA*, Tomofumi MARUTA, Yong LIU, Tomoaki MIYAO, Yusuke KAWANE, Nobuo OUCHI, Hidetomo OGURI, Masanori IKEGAMI¹, and Kazuo HASEGAWA

J-PARC Center, Tokai, Ibaraki 319-1195, Japan

¹ *FRIB, Michigan State University, East Lansing, MI 48824-1321, USA*

E-mail: akihiko.miura@j-parc.jp

(Received: September 10, 2014)

In 2009, Japan Proton Accelerator Research Complex (J-PARC) began a project to upgrade the J-PARC Linac using the annular-ring coupled structure linac cavities. The aim was to achieve a beam power of 1 MW at the exit of the downstream rapid cycling synchrotron. For the upgraded beam line, beam monitors were designed, fabricated, and laid out considering the beam commissioning strategy. This study introduces the beam monitor layout in the new beam line and the results of commissioning, which confirm appropriate functioning of the beam monitors.

KEYWORDS: J-PARC, Linac, Energy Upgrade, Beam Monitor, Beam Commissioning

1. Introduction

The Japan Atomic Energy Agency (JAEA) and the High Energy Accelerator Research Organization (KEK) have managed the Japan Proton Accelerator Research Complex (J-PARC) project at the JAEA Tokai site since 2001 [1, 2]. The beam commissioning of linac began in 2006, and since then, a 181 MeV beam was injected into the downstream 3 GeV rapid cycling synchrotron (RCS). Since the beginning of J-PARC, user operation has been continuous with the exception of a 10-month hiatus due to the Tohoku earthquake, which occurred in 2011. In parallel with the 181 MeV beam operation, J-PARC began a 400 MeV energy upgrade project and an improvement of front end for 50 mA peak current operation, including the 50 mA ion source, the radio frequency quadrupole (RFQ) linac, and the corresponding beam line in 2009. The aim was to obtain an RCS beam power of 1 MW. New annular-ring coupled structure (ACS) linac cavities were developed for this energy upgrade project [3]. In addition, beam monitors were designed and fabricated to accommodate the new beam parameters. The new beam monitors were completely fabricated as of the end of 2012. During the shutdown from August to mid-November 2013, we installed ACS cavities and beam monitors. We started beam commissioning in December 2013 to obtain a beam energy of 400 MeV. During the shutdown from July to September 2014, we exchanged the front end equipment. In this study, we introduce the layout of the new beam monitors and describe the methods used for beam commissioning and the results obtained, which

confirm appropriate functioning of the beam monitors.

2. New Beam Monitor Layout for 400 MeV Linac Beam Line

2.1 Beam Line before and after Upgrade

The J-PARC Linac originally consisted of a 50 keV negative hydrogen ion source, a 3 MeV RFQ, a 50 MeV drift tube linac (DTL), and a 181 MeV separated-type DTL (SDTL) [2]. We had two SDTL-type debunchers allocated at an ACS section and a linac-to-3-GeV RCS beam transport (L3BT). In the energy upgrade project, we moved the two original debuncher cavities to the end of the SDTL section to form the sixteenth acceleration module of SDTL cavities, which increases beam energy to 191 MeV. We installed new ACS-type bunchers for longitudinal matching between the SDTL and ACS cavities, because the operating frequency of ACS is 972 MHz, which is a threefold jump from the frequency of SDTL.

Numerous beam monitors were used in the original beam line, such as the beam position monitor (BPM) to measure the beam orbit, the beam current monitor (slow current transformer (SCT)) to measure the beam current, the beam phase monitor (fast current transformer (FCT)) to tune the phase and voltage of the acceleration field (phase scan), the transverse profile monitor (wire scanner monitor (WSM)) to mitigate the transverse mismatching, and the beam loss monitor (BLM). These beam monitors are essential for tuning accelerator devices, maintaining beam quality, mitigating beam loss, and monitoring operational status [4]. The energy upgrade project involved installing or replacing a total of 49 BPMs, 52 FCTs, 24 SCTs, 4 WSMs, and 24 BLMs. Most of the monitors in the original L3BT will continue to be used after the energy upgrade.

2.2 Installation of Beam Monitors in each ACS Module

Figure 1 shows a detailed layout of the beam monitors in each ACS module. Each module consists of two accelerating cavities and a bridge coupler. They contain a drift space in which the quadrupole doublets are placed at the bridge coupler. Another drift space exists between the modules, where most of the beam monitors are installed. We use the time-of-flight (TOF) method to measure the beam energy at the drift space without any acceleration devices. To do this, a pair of FCTs is located at the exit of the

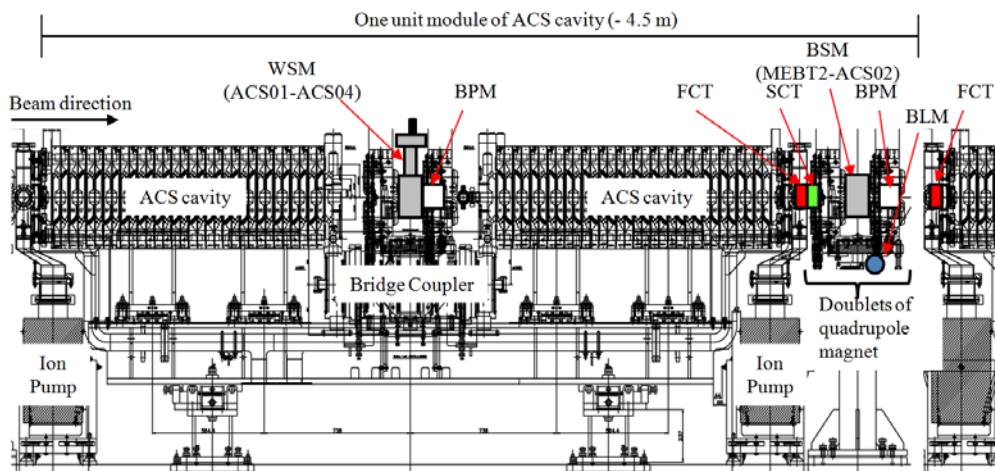


Fig. 1. Periodical beam monitor layout of all ACS cavities. MEBT2 is the second medium energy beam transport between SDTL and ACS, and BSM is the bunch shape monitor.

second cavity and at the entrance of the next cavity. The distance between each member of the pair normally corresponds to $2.5\beta\lambda$, where β is the relative velocity and λ is the wavelength of the acceleration RF. However, we referred to the distal combination of FCTs, which corresponded to $21\beta\lambda$ [5]. SCT and FCT are in a single vacuum chamber package, where SCT is located behind FCT to measure the beam current. Because the dynamic range of SCT is from 0.1 to 100 mA, the beam transmission through the acceleration module can be obtained by comparing it with the beam current measured by the upstream and downstream SCTs. BPM is mounted directly on the yoke of the quadrupole magnet (QM) to improve its position accuracy with respect to the position of QM. BPM installed on the bridge coupler is used as a backup. We use BPM between the cavities to correct the beam orbit. BLM location was optimized by verification under beam operation because, during beam operation, BLM should be optimized to suppress a background X-rays from the RF cavities. Finally, we installed BLM heads at the downstream edge of the magnet tables.

This layout was adopted for all ACS modules with the addition of WSM or bunch shape monitor (BSM) for some of the upstream modules.

2.3 Beam Monitor Layout Upstream of a new ACS Section

Figure 2 shows the beam monitor layout around SDTL16, which is the last SDTL cavity of the energy upgraded linac. It has 12 QMs in the second medium energy beam transport (MEBT2) between SDTL and ACS, eight of which are destined for use for transverse matching. Four WSMs were installed between the doublets of QMs on the bridge coupler of the first four ACS modules. Furthermore, from MEBT2 to ACS02, three BSMs are located in a space between the downstream doublets of the module, where the gate valve is usually positioned. The strength of the quadrupole doublets was adjusted to ensure the matching of the measured root mean square (RMS) beam widths in the WSM array. At least three WSMs are required to do this tuning, with the one remaining WSM installed for redundancy. We plan to adopt a similar scheme for the longitudinal matching using three BSMs installed periodically upstream of the ACS section, i.e., between the end of MEBT2 and ACS02. The amplitude of two of these bunchers is adjusted to ensure the matching of the measured RMS beam widths for the

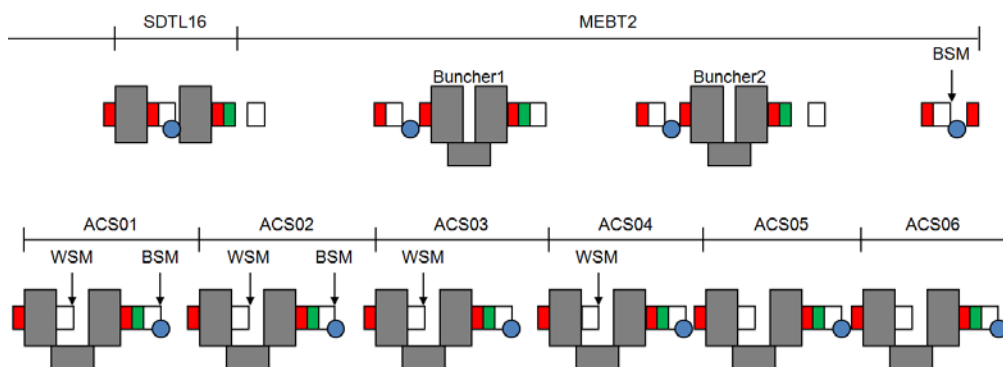


Fig. 2. Beam monitor layout around SDTL16, matching section between SDTL and ACS (MEBT2), and upstream part of ACS section after energy upgrade. The gray squares represent the cavities, the white squares represent BPMs, the red squares represent FCTs, and the green squares represent SCTs. Blue circles are BLMs, and the position of WSMs and BSMs are indicated by arrows.

BSM array. BSMs were scheduled to be installed in the 181 MeV beam line, but the installation was postponed due to vacuum problems.

3. Beam Commissioning for Confirmation of Beam Monitor Functioning

3.1 Commissioning Plans after Upgrade

The original linac accelerated a negative hydrogen ion beam for injection into RCS at 181 MeV. This energy increased to 400 MeV after we installed the ACS cavities. The commissioning, which began in mid-December 2013, had two important missions: (1) establish 400 MeV operation and (2) determine the suitable parameters for high-power beam operation (i.e., output power of 1 MW). Before attaining 400 MeV operation, we had to deal with two other missions for beam commissioning: to reproduce 181 MeV operation again in the new beam line and to confirm the proper functioning of beam monitors destined for tuning the ACS cavities [6]. During the first week of beam commissioning, we completed the first mission. In doing so, we continuously confirmed appropriate functioning of the beam monitors.

3.2 Confirmation of Beam Monitor Functioning

We confirmed appropriate functioning and alignment offset of BPMs using the conventional beam-based calibration (BBC) method, which involves examining the responses to a change in the strength of the QMs or steering magnets [7]. This method requires using a singlet QM and one of its upstream steering magnets as tuning knobs. The offset of the magnetic center is extracted by analyzing the deviation of the beam orbit generated by varying QM and the steering magnet. The beam orbit is measured using BPM nearby QM and a downstream BPM. In practice, to determine the BPM with the best response, several downstream BPMs are used for the measurement. Because the beam line and magnet layout were completely changed after SDTL16, we used this method to check the alignment errors from SDTL16 to the end of MEBT2. Consequently, the offset was measured to be 18.8 μm with an accuracy of a few tens of micrometers.

We also checked the functioning of FCTs while delivering the 181 MeV beam to the straight beam dump. Because the bunch structure of the beam could be reasonably sustained over the new ACS section, we could measure the beam energy with various FCT pairs using the TOF method. The beam energies measured with the different FCT pairs should agree to within the expected accuracy for the TOF method, considering deceleration by exciting idle cavities. In the beam phase measurement, we accounted for the calibration with phase offsets from FCT itself and from the signal transmission line. After tuning the SDTL cavities, we used the 181 MeV beam to compare various FCT pairs for the energy measurement. If the calibration of the offset value is appropriately adjusted to the 324 MHz reference, the output energy should be 181 MeV with errors of 1.0%. All data, with only one exception, were obtained within 0.6% (with a corresponding beam energy of 1.0 MeV) upon repeated calibrations. Most importantly, the FCT pair can be used for the phase scan because of the good energy measurement. The proper amplitude and phase of each accelerating cavity of ACS were set by the phase scan method [5]. In the phase scan method, the beam energy was measured by the TOF method with a pair of FCTs. An example of the phase scan result acquired at

ACS20 appears in Fig. 3. The measured energy and simulation results are consistent. The tuning error is within 1.0% in amplitude and 1° in phase. The measured beam energy at the ACS section after the phase scan agrees well with the design energy, with a difference of only 0.6% over the entire ACS section. The output energy measured at the last ACS cavity was 400.4 MeV, which is 0.10 % higher than the design value. We also checked for consistency with another energy measurement by BPM. In the L3BT-arc section is the largest dispersion point in the linac. The magnetic field is adjusted to the calculated value for the suitable beam orbit at 400 MeV. When the beam energy is shifted from 400 MeV, the beam orbit is also shifted. The corresponding energy accuracy is approximately 1.0%, because the positional accuracy of BPM is less than 0.1 mm. The measurement of the beam orbit at the largest dispersion point indicates that the energy shift is within 0.8%, which is below the lowest limit of this method. After we injected the 400 MeV beam into RCS, the corresponding beam energy was measured by the closed-orbit distortion method. According to this measurement, the energy shift is only 0.21%.

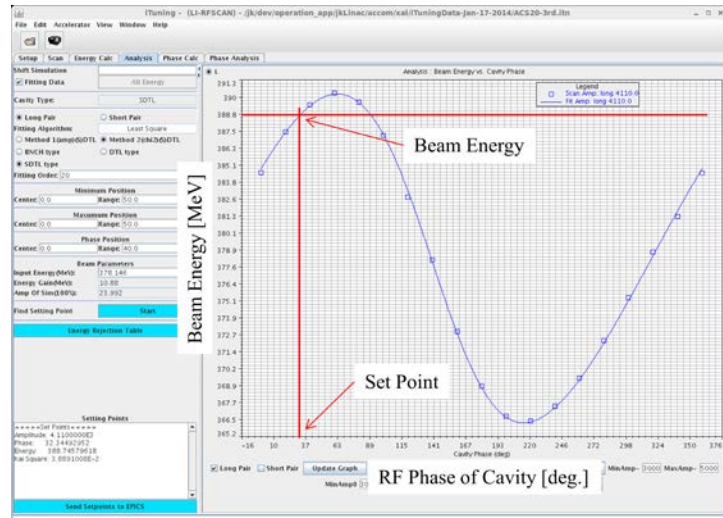


Fig. 3. Example of phase scan result taken at ACS20 (at January 17, 2014). Dots are the measurement points taken with 20° intervals, and curve is the simulation result.

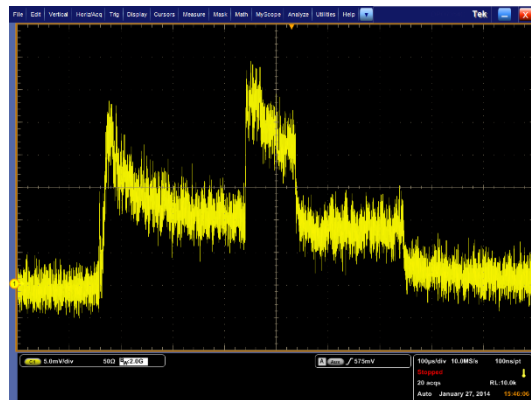
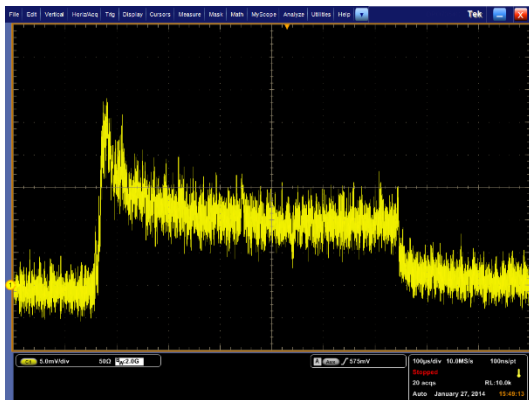


Fig. 4. Beam loss signal acquired at ACS18, where higher beam loss can be observed (data acquired on January 27, 2014). Left side shows a BLM signal with no beam, and right side shows A BLM signal with the beam. X-ray signals generated from RF cavities are both observed, and the real beam loss is clearly observed in the middle of the signal. In the panels, the horizontal axis is 100 μ s/div, and the vertical axis is 5.0 mV/div. A RF width is approximately 650 μ s, and a beam pulse width is 100 μ s without chopping.

BLMs were removed once for the installation work, but we reinstalled the same BLM heads in almost the same configuration. During the experiment, BLMs were sensitive to X-rays emitted from the RF cavities. The left panel of Fig. 4 shows the response from BLM in ACS18 with RF “on” but without the beam. When the beam is “on,” the signal waveform changes to the correct waveform. Actual beam loss is the difference between beam “on” and “off.” This situation can be acceptable for beam tuning, but the background X-rays cannot be neglected. The BLM position was optimized by this verification during beam operation because BLM is sensitive to X-rays released from acceleration cavities, and the real beam loss signal might be difficult to discern amidst a high X-ray background. BLM is between the iron plates of the magnet support tables to prevent it from being directly exposed to X-rays from RF cavities. We will also use the scintillation BLM, which is selectively sensitive to γ rays from actual beam loss, to clarify the beam loss mechanism [4].

4. Summary

A 400 MeV energy upgrade project for the J-PARC Linac began in 2009. In parallel with the development of the new cavity for the energy upgrade project, beam monitors for beam commissioning were designed and fabricated. During the shutdown from August to mid-November 2013, we installed the newly fabricated beam monitors in the new beam line with new ACS cavities.

The beam commissioning started in mid-December 2013 and ran to mid-January 2014. During the first stage of commissioning, based on our experience, we achieved 181 MeV operation. Before attaining 400 MeV operation, we confirmed appropriate functioning of BPMs, beam phase monitors, beam profile monitors, and BLMs, while delivering the 181 MeV beam to the straight beam dump. The BBC measurement of BPM in MEBT2, the position of BPMs, and the corresponding QMs are acceptable (only small mechanical offsets). The beam energy was measured using new pairs of FCTs in a new ACS beam line. Because the measurement accuracy was kept under 0.6%, we could use the phase scan of appropriate setting of ACS cavities to establish 400 MeV operation. After establishing 400 MeV operation, we confirmed the beam energy using two approaches: the TOF method involving the new pair of FCTs and by detecting the beam orbit at the largest dispersion point using BPMs. Although the X-ray background was not perfectly suppressed, a clear beam loss signal was observed, which indicates that we can use these BLMs to continuously tune the linac.

References

- [1] Y. Yamazaki: Proc. of PAC 2003 (Portland, 2003), p. 576.
- [2] Y. Yamazaki ed.: "Technical Design Report of J-PARC", KEK Report 2002-12 (2003).
- [3] H. Oguri, et. al.: Proceedings of IPAC2013, Shanghai, China, WEYB101, 2013.
- [4] A. Miura, et. al.: Proceedings of IBIC2012, Tsukuba, Japan, MOIA02, 2012.
- [5] G. Shen, et. al.: Proc. of PAC07, TUPAN062, Albuquerque, New Mexico, USA, 2007.

- [6] M. Ikegami, et. al.: Proceedings of IPAC13, Shanghai, China, THPWO028, 2013.
- [7] G. Shen, et. al.: Proc. of the 4th Annual Meeting of Particle Accelerator Society of Japan, and the 32nd Linear Accelerator Meeting in Japan, TP60, Wako Japan, 2007 (in English)
- [8] M. Ikegami, et. al.: Proc. of PAC07, p. 1481, Albuquerque, New Mexico, USA, 2007.
- [9] H. Sako, et. al.: Proc. of PAC07, p. 257, Albuquerque, New Mexico, USA, 2007.